



Cite this: *Org. Biomol. Chem.*, 2023, **21**, 8079

Received 30th August 2023,
 Accepted 19th September 2023

DOI: 10.1039/d3ob01385e

rsc.li/obc

Rod-like nanostructures through amphiphilic OPE-porphyrin self-organization†

Chiara M. A. Gangemi,[‡] Maria A. Castriciano,[‡] Ester D'Agostino,[‡] Andrea Romeo,[‡] Paola M. Bonaccorsi,[‡] Anna Barattucci[‡]* and Luigi Monsù Scolaro[‡]*

A new amphiphilic monosubstituted porphyrin functionalized by a β-D-glucoside terminated oligophenylenethylen (OPE) able to self-arrange into nano-aggregates in polar solvents has been synthesized and fully characterized in its monomeric and aggregated forms.

Non-covalent multichromophoric assemblies are highly investigated due to their involvement either in many fundamental processes, such as photosynthesis,¹ or applications such as photodynamic therapy (PDT)² or photovoltaics.³ In biological processes, the requirement for vectorial processes, *i.e.* energy and/or electron transfer, is rigidity and fixed geometry among the various components, usually accomplished through embedding the species in bilayer lipid membranes or protein scaffolds. In this respect, several chromophore-based systems have been proposed and complex architectures have been realized through self-assembling processes, exploiting a variety of specific interactions.⁴ Porphyrins are a large class of natural and synthetic compounds that have been widely used as versatile building blocks. They possess an extended aromatic region with peculiar electronic features, dominated by very intense absorption bands in the visible range of the spectrum (B- and Q-bands) and usually intense fluorescence emission.^{5,6} Self-aggregation can spontaneously occur depending on a variety of

non-covalent interactions, generally dominated by π -stacking. The electronic coupling between adjacent chromophores depends on the geometrical arrangement of the interacting chromophores, classified into H-type (face-to-face) or J-type (edge-to-edge) dispositions, exhibiting bands shifted to higher and lower energies, respectively.⁷ Intriguing new properties could be added to supramolecular species by introducing appropriate pendant moieties at the periphery of these compounds:^{8–11} (i) charged or ionisable groups allow electrostatic contacts, driving the formation of even extended aggregates, such as in the case of J-aggregates of sulphonatophenyl porphyrins^{12–15} and (ii) carbohydrates could promote hydrogen bonding interactions and potentially induce chirality in eventual supramolecular assemblies.¹⁶ In this respect, the choice of good solvent/poor solvent mixtures allows for achieving a variety of nanostructures, depending on various parameters, including the ratio and shape of the hydrophobic *vs.* hydrophilic parts. Also in an aqueous environment, the medium properties in terms of pH and/or ionic strength, together with the temperature, have a deep impact on the kinetics and the final nano-architecture.¹⁷ Furthermore, since carbohydrate-recognized proteins are usually overexpressed on the membrane of certain tumor cells, the introduction of one^{18–23} up to four sugar moieties on a porphyrin has led to several targeted PDT applications.^{24–27} Another interesting class of chromophores are oligo-phenylene-ethynylenes (OPEs). These systems have been widely exploited as rigid spacers able to electronically couple acceptor and donor supramolecular porphyrinoid based dyads^{28–30} or to provide optimal separation in self-assembled monolayers³¹ or in semiconductor nanoparticles for electronic applications.³² An appropriate functionalization with carbohydrates affords systems with potential application in photodynamic therapy,^{33–36} such as fluorescent biomarkers^{37,38} or inhibitors of bacterial growth.³⁹ To the best of our knowledge, only one example has been reported so far in the literature on the synthetic procedure coupling a monosubstituted porphyrin with a carbohydrate moiety through an OPE based bridge.⁴⁰

Dipartimento di Scienze Chimiche, Biologiche, Farmaceutiche ed Ambientali, Università degli Studi di Messina, V.le F. Stagno D'Alcontres 31, 98166 Messina, Italy. E-mail: lmonsu@unime.it

†Electronic supplementary information (ESI) available: Fig. S1–S8: ¹H and ¹³C NMR spectra; Fig. S9–S11: ESI mass spectra; Fig. S12: Absorption spectra of GAP in chloroform and Beer's plot; Fig. S13: Absorption and emission spectra of GAP in chloroform; Fig. S14: Excitation and emission spectra of OPE in chloroform; Fig. S15: CD spectrum of GAP in chloroform; Fig. S16: Absorption spectra of GAP in chloroform, chloroform/methanol 50/50 v/v, and methanol; Fig. S17: RLS spectra of GAP in methanol and water/methanol 40/60 v/v. Fig. S18: DLS distribution of GAP in water/methanol 40/60 v/v; Fig. S19: Absorption spectrum of GAP in water/methanol 40/60 v/v and in the presence of KI; and Fig. S20: AFM image and relative profile of GAP aggregates on a silicon surface. See DOI: <https://doi.org/10.1039/d3ob01385e>

‡These authors contributed equally.

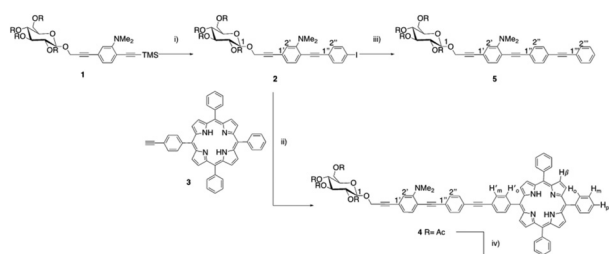


Hence, on these premises, we designed a new amphiphilic system consisting of a free-base porphyrin macrocycle, mono-substituted at the meso-position by an oligophenyleneethylene (OPE) moiety bearing a dimethylamino substituent at one of the aromatic residues and a β -D-glucoside termination.^{33,35} The introduction of the hydrophilic sugar termination, together with the ionisable group, was intended to study the supramolecular behaviour of the amphiphilic species for the construction of new biocompatible aggregates. The OPE residue was chosen for a dual purpose: (i) to use the conjugated fragment as a spacer between the two functional groups of the amphiphilic system^{33–36} and, (ii) as a chromophore, to study the mutual influence and the potential communication between the porphyrin and the OPE residues. The strategy employed for the synthesis of the bis-chromophoric system GAP (Scheme 1) involves the step-by-step modular approach to the preparation of the OPE chain. Starting from aminoaryl sugar derivative **1**,³⁵ the conjugated chain elongation to **2** was realized through Pd(0) mediated cross-coupling with an excess of 1,4-diiodobenzene and in the presence of a stoichiometric amount of Ag₂O. The last reactant is reported to cause *in situ* direct desilylation of the terminal acetylenic residue,⁴¹ so avoiding the alternative use of basic conditions for deprotection,⁴² also responsible for the undesired deacetylation of the sugar residue that could cause low solubility in polar organic solvents. The reaction was complete in 1.5 hours and the iodoarene **2** was obtained in 60% yield.

Copper-free Heck–Cassar–Sonogashira cross-coupling of **2** with monofunctionalized porphyrin **3**^{42,43} leads to chromophore **4**, and then quantitatively deprotected to amphiphilic GAP using an aqueous ammonia solution in THF/MeOH. Finally, the trimeric OPE **5** was synthesized as a model compound for the spectroscopic characterization of **4** and GAP. The cross-coupling of **2** with an excess of commercial phenylacetylene afforded **5** in almost quantitative yields. Due to its amphiphilic nature the complete characterization of GAP was conducted in a CDCl₃/CD₃OD mixture (13 : 1, see ESI, Fig. S1–S11†). The absorption spectra of GAP were recorded in chloroform wherein no aggregation occurred as confirmed by the linearity of Beer's law ($\epsilon_{421 \text{ nm}} = 3.25 \times 10^5 \text{ M}^{-1} \text{ cm}^{-1}$) (see ESI, Fig. S12†) and by the resonance light scattering (RLS) profile,

which is comparable in intensity with the neat solvent (data not shown). A typical absorption spectrum (see ESI, Fig. S13†) mainly exhibits features of the porphyrin moiety in the visible range with a B-band located at 421 nm accompanied by four Q-bands at 517, 552, 591, and 647 nm. However, the presence of the OPE unit can be assessed by an additional low intensity feature in the UV region as confirmed by the spectroscopic behaviour of the trimeric OPE **5** taken as a reference (see ESI, Fig. S14†). The circular dichroism (CD) spectrum shows no induced CD signal in the porphyrin absorption region indicating no coupling with the chiral sugar residue in the side chain on the aromatic ring (see ESI, Fig. S15†). GAP is strongly emissive in solution and its calculated fluorescence quantum yield value ($\Phi = 0.033$ in CHCl₃) is comparable with that reported in the literature for similar porphyrins.⁴⁴ The fluorescence emission spectrum displays the typical two-banded pattern (654 and 718 nm) and the emission decay shows a mono-exponential profile with a long-living lifetime value (8 ns) ascribable to the porphyrin in its monomeric form.⁵ In order to tune the extent of aggregation, which is well known to strongly depend on the nature of the media, we investigated the system on increasing the polarity of the solvent moving from chloroform to methanol (CHCl₃/MeOH, 50/50 v/v and pure MeOH). In these solvents, the spectra remain substantially unchanged exhibiting only a slight hypsochromic shift of the B-band with respect to CHCl₃ due to the less hydrophobic environment around the porphyrin ($\Delta\lambda = -3 \text{ nm}$ and -6 nm , respectively; see ESI, Fig. S16†).⁵

Evident spectroscopic changes have been observed when methanol/water at different v/v ratio values are used as solvents. More specifically, as shown in Fig. 1, the addition of increasing amounts of water to a porphyrin solution in methanol, up to a 40/60 water/methanol (v/v) ratio, induces a consistent bathochromic shift ($\Delta\lambda = +16 \text{ nm}$) together with a concomitant broadening of the B-band. The corresponding fluorescence emission spectra display a substantial quenching with respect to the sample in pure methanol in line with the fluorescence emission intensity decays that show a bi-exponential behaviour with two lifetime values of 1.6 ns (relative amplitude 80%) and 5.6 ns (relative amplitude 20%), respectively. The RLS spectrum exhibits a peak in proximity to the main



Scheme 1 Synthetic route to GAP. (i) 1,4-Diiodobenzene, Pd(PPh₃)₄, Ag₂O, THF/DMF (1/1), 60 °C, 1 h 30 min; (ii) Pd(PPh₃)₄, Et₃N, DMF, 70 °C, 1 h 30 min; (iii) ethynylbenzene, Pd(PPh₃)₄, Et₃N, DMF, 70 °C, 2 h; and (iv) NH₄OHaq, MeOH/THF (1/1), RT, overnight.

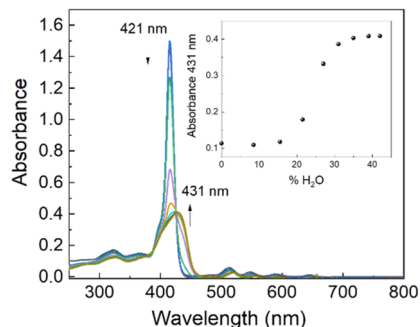


Fig. 1 UV/Vis spectral change of GAP in methanol on increasing the water percentage (v/v). GAP in methanol. [GAP] = 7 μM , $T = 298 \text{ K}$.



absorption band indicating the presence of aggregated species (see ESI, Fig. S17†). According to RLS theory, this spectroscopic evidence suggests that the aggregates should be constituted by at least 25 interacting porphyrin units, with a strong coupling among their electronic transition moments.^{45,46} This hypothesis has been definitively confirmed by dynamic light scattering (DLS) measurements which reveal the presence of well-dispersed nanometer-sized porphyrin aggregates ($R_H = 200 \pm 50$ nm; see ESI, Fig. S18†).

Depolarized RLS measurements can give useful insights into the geometrical disposition of the chromophores in large aggregates. The value of the depolarization ratio $\rho\nu(90)$ calculated for the investigated samples is 0.125, from which a slip angle $\varphi = 40$ or 50° between adjacent porphyrin planes can be calculated, assuming a parallel arrangement of the transition moments of the exciton-coupled chromophores (Fig. 2a).⁴⁵ This angle is in line with the observed J-type shift of the B-band to a lower energy with respect to the isolated monomer. Considering also that these aggregates are CD silent (data not shown), a tilt angle close to 90° could be envisaged between the transition moments (Fig. 2b).⁴⁷ The presence of supramolecular aggregates in solution is ascribable to the ability of both porphyrins and OPEs to establish π -stacking interactions together with the presence of free glucosidic units, which allow, in principle, the formation of intermolecular hydrogen bonds that stabilize the porphyrin network.

To clarify the nature of these aggregates, HCl (up to 0.1 M) was added to the 40/60 water/methanol solution. The unchanged spectroscopic features suggest that the hydrophobic porphyrin core is located within, which conversely exposes the hydrophilic glycosidic part towards the aqueous environment. Fluorescence emission experiments, performed by adding an iodide anion as a quencher, confirm this hypothesis.⁴⁸ Indeed, the addition of the quencher induces only a slight bathochromic shift of the UV/Vis profile without affecting the fluorescence emission in terms of intensity and lifetimes (see ESI, Fig. S19†). Finally, a 40/60 water/methanol solution of GAP was dropped onto the silicon surface. After evaporation of the solvent, AFM microscopy (Fig. 3) shows well-defined rod-like structures with an average diameter of about 50 nm, a length of 300 nm and a thickness of about 20 nm (see ESI, Fig. S20†), in agreement with the size

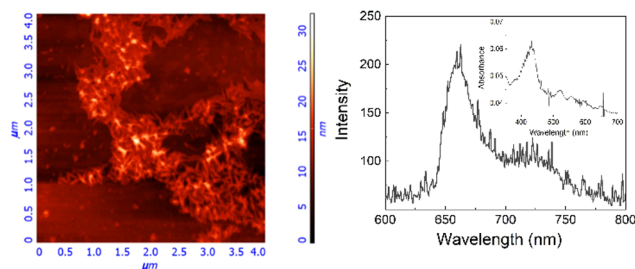


Fig. 3 AFM image of the silicon surface (left) and fluorescence emission and absorption spectra (right and inset) of GAP aggregates. 1 μ M GAP in 40/60 v/v water/methanol added dropwise and evaporated at room temperature on the silicon surface (left) and glass surface (right), λ_{ex} 430 nm.

measured in solution. Considering that the calculated length of a single GAP unit from molecular models is around 3.9 nm, all the previous experimental evidence suggest that these nanoaggregates cannot be formed by a single stacked arrangement as shown in the model of Fig. 2b. Assuming a typical inter-porphyrin distance of 0.33–0.35 nm, a complete turn of the sugar pendant arms occurs with a pitch of *ca.* 1 nm. Therefore, hydrogen-bonding interactions among these moieties could be operative to bridge or interdigitate more porphyrin stacks to justify the observed diameter of the final structures.

In conclusion, we have designed, synthesized, and fully characterized a new amphiphilic monosubstituted porphyrin functionalized by an oligophenyleneethylene (OPE) with a β -D-glucoside termination. The introduction of an OPE and a hydrophilic sugar moiety at the periphery allowed the induction of the supramolecular organization of the amphiphilic species on increasing the polarity of the medium, thus affording new promising biocompatible nano-aggregates, potentially suitable for photodynamic therapy, bioimaging or drug delivery.

Conflicts of interest

There are no conflicts to declare.

Acknowledgements

The authors thank Prof. Salvatore Patanè for AFM microscopy. The work was financially supported by the European Union-FSE-REACT-EU, PON Research and Innovation 2014–2020 DM.1062/2021 and Next Generation EU, PNRR Samothrace Project (ECS00000022).

References

- 1 S. Y. Cao, A. Roslawska, B. Doppagne, M. Romeo, M. Feron, F. Cherioux, H. Bulou, F. Scheurer and G. Schull, *Nat. Chem.*, 2021, **13**, 766–770.

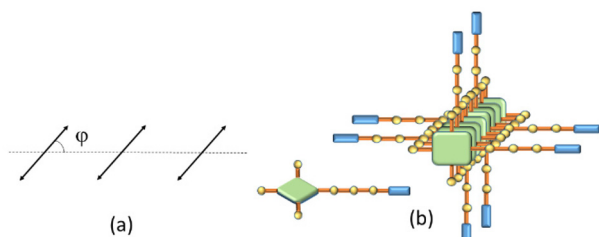


Fig. 2 Model for (a) the geometrical arrangement showing the slip angle φ between the transition moments and the line connecting the centroids of the porphyrin rings, and (b) sketch of the porphyrin stacks.



- 2 L. X. Sun, J. Wang, B. C. Yang, X. X. Wang, G. X. Yang, X. Q. Wang, Y. Y. Jiang, T. Y. Wang and J. Z. Jiang, *RSC Adv.*, 2021, **11**, 10061–10074.
- 3 G. Charalambidis, K. Karikis, E. Georgilis, B. L. M'Sabah, Y. Pellegrin, A. Planchat, B. Lucas, A. Mitraki, J. Boucle, F. Odobel and A. G. Coutsolelos, *Sustainable Energy Fuels*, 2017, **1**, 387–395.
- 4 J.-H. Fuhrhop and J. Köning, *Membranes and Molecular Assemblies: The Synkinetic Approach*, The Royal Society of Chemistry, Cambridge, 1994, DOI: [10.1039/9781847551368-fp001](https://doi.org/10.1039/9781847551368-fp001).
- 5 N. C. Maiti, M. Ravikanth, S. Mazumdar and N. Periasamy, *J. Phys. Chem. B*, 1995, **99**, 17192–17197.
- 6 W. I. White, *The Porphyrins*, Academic Press, New York, 1978.
- 7 E. G. McRae and M. Kasha, *Physical Processes in Radiation Biology*, Academic Press, New York, 1964.
- 8 C. M. A. Gangemi, R. Randazzo, M. E. Fragalà, G. A. Tomaselli, F. P. Ballistreri, A. Pappalardo, R. M. Toscano, G. Trusso Sfrazzetto, R. Purrello and A. D'Urso, *New J. Chem.*, 2015, **39**, 6722–6725.
- 9 M. A. Castriciano, R. Zagami, M. Trapani, A. Romeo, S. Patane and L. M. Scolaro, *Chirality*, 2015, **27**, 900–906.
- 10 M. A. Castriciano, A. Romeo, N. Angelini, N. Micali, A. Longo, A. Mazzaglia and L. M. Scolaro, *Macromolecules*, 2006, **39**, 5489–5496.
- 11 L. M. Scolaro, C. Donato, M. Castriciano, A. Romeo and R. Romeo, *Inorg. Chim. Acta*, 2000, **300**, 978–986.
- 12 A. Romeo, M. A. Castriciano, I. Occhiuto, R. Zagami, R. F. Pasternack and L. M. Scolaro, *J. Am. Chem. Soc.*, 2014, **136**, 40–43.
- 13 R. Zagami, A. Romeo, M. A. Castriciano and L. M. Scolaro, *J. Mol. Liq.*, 2021, **332**, 115801.
- 14 R. Zagami, A. Romeo, M. A. Castriciano and L. Monsù Scolaro, *Chem. – Eur. J.*, 2017, **23**, 70–74.
- 15 R. Zagami, M. A. Castriciano, A. Romeo, M. Trapani, R. Pedicini and L. M. Scolaro, *Dyes Pigm.*, 2017, **142**, 255–261.
- 16 M. Stefanelli, F. Mandoj, G. Magna, R. Lettieri, M. Venanzi, R. Paolesse and D. Monti, *Molecules*, 2020, **25**, 4544.
- 17 R. Zagami, M. A. Castriciano, A. Romeo and L. M. Scolaro, *J. Porphyrins Phthalocyanines*, 2023, **27**, 463–470.
- 18 J. P. C. Tome, E. M. P. Silva, A. Pereira, C. M. A. Alonso, M. A. F. Faustino, M. Neves, A. C. Tome, J. A. S. Cavaleiro, S. A. P. Tavares, R. R. Duarte, M. F. Caeiro and M. L. Valdeira, *Bioorg. Med. Chem.*, 2007, **15**, 4705–4713.
- 19 J. P. C. Tome, M. Neves, A. C. Tome, J. A. S. Cavaleiro, A. F. Mendonca, L. S. N. Pegado, R. Duarte and M. L. Valdeira, *Bioorg. Med. Chem.*, 2005, **13**, 3878–3888.
- 20 F. Giuntini, F. Bryden, R. Daly, E. M. Scanlan and R. W. Boyle, *Org. Biomol. Chem.*, 2014, **12**, 1203–1206.
- 21 F. Figueira, L. M. O. Lourenco, M. Neves, J. A. S. Cavaleiro and J. P. C. Tome, *J. Porphyrins Phthalocyanines*, 2020, **24**, 330–339.
- 22 A. Fadlan, H. Tanimoto, T. Ito, Y. Aritomi, M. Ueno, M. Tokuda, S. Hirohara, M. Obata, T. Morimoto and K. Kakiuchi, *Bioorg. Med. Chem.*, 2018, **26**, 1848–1858.
- 23 M. C. Bennion, M. A. Burch, D. G. Dennis, M. E. Lech, K. Neuhaus, N. L. Fendler, M. R. Parris, J. E. Cuadra, C. F. Dixon, G. T. Mukosera, D. N. Blauch, L. Hartmann, N. L. Snyder and J. V. Ruppel, *Eur. J. Org. Chem.*, 2019, 6496–6503.
- 24 X. Zheng and R. K. Pandey, *Anticancer Agents Med. Chem.*, 2008, **8**, 241–268.
- 25 S. Singh, A. Aggarwal, N. Bhupathiraju, G. Arianna, K. Tiwari and C. M. Drain, *Chem. Rev.*, 2015, **115**, 10261–10306.
- 26 M. Rosa, N. Jedryka, S. Skorupska, I. Grabowska-Jadach and M. Malinowski, *Int. J. Mol. Sci.*, 2022, **23**, 11321.
- 27 M. Lupu, P. Maillard, J. Mispelter, F. Poyer and C. D. Thomas, *Photochem. Photobiol. Sci.*, 2018, **17**, 1599–1611.
- 28 A. Lembo, P. Tagliatesta, D. M. Guldi, M. Wielopolski and M. Nuccetelli, *J. Phys. Chem. A*, 2009, **113**, 1779–1793.
- 29 E. Goransson, J. Boixel, J. Fortage, D. Jacquemin, H. C. Becker, E. Blart, L. Hammarstrom and F. Odobel, *Inorg. Chem.*, 2012, **51**, 11500–11512.
- 30 M. P. Eng, J. Martensson and B. Albinsson, *Chem. – Eur. J.*, 2008, **14**, 2819–2826.
- 31 S. Watcharinyanon, D. Nilsson, E. Moons, A. Shaporenko, M. Zharnikov, B. Albinsson, J. Martensson and L. S. O. Johansson, *Phys. Chem. Chem. Phys.*, 2008, **10**, 5264–5275.
- 32 J. Rochford and E. Galoppini, *Langmuir*, 2008, **24**, 5366–5374.
- 33 A. Lara-Pardo, A. Mancuso, S. Simon-Fuente, P. M. Bonaccorsi, C. M. A. Gangemi, M. A. Moline, F. Puntoriero, M. Ribagorda, A. Barattucci and F. Sanz-Rodriguez, *Org. Biomol. Chem.*, 2023, **21**, 386–396.
- 34 C. M. A. Gangemi, A. Barattucci and P. M. Bonaccorsi, *Molecules*, 2021, **26**, 3088.
- 35 E. Deni, A. Zamarron, P. Bonaccorsi, M. C. Carreno, A. Juarranz, F. Puntoriero, M. T. Sciortino, M. Ribagorda and A. Barattucci, *Eur. J. Med. Chem.*, 2016, **111**, 58–71.
- 36 A. Barattucci, E. Deni, P. Bonaccorsi, M. G. Ceraolo, T. Papalia, A. Santoro, M. T. Sciortino and F. Puntoriero, *J. Org. Chem.*, 2014, **79**, 5113–5120.
- 37 A. Mancuso, A. Barattucci, P. Bonaccorsi, A. Giannetto, G. La Ganga, M. Musarra-Pizzo, T. M. G. Salerno, A. Santoro, M. T. Sciortino, F. Puntoriero and M. L. Di Pietro, *Chem. – Eur. J.*, 2018, **24**, 16972–16976.
- 38 E. Arias, M. T. Mendez, E. Arias, I. Moggio, A. Ledezma, J. Romero, G. Margheri and E. Giorgetti, *Sensors*, 2017, **17**, 1025.
- 39 F. Pertici, N. Varga, A. van Duijn, M. Rey-Carrizo, A. Bernardi and R. J. Pieters, *Beilstein J. Org. Chem.*, 2013, **9**, 215–222.
- 40 B. Godlewski, D. Baran, M. de Robichon, A. Ferry, S. Ostrowski and M. Malinowski, *Org. Chem. Front.*, 2022, **9**, 2396–2404.
- 41 A. Mori, T. Kondo, T. Kato and Y. Nishihara, *Chem. Lett.*, 2001, 286–287, DOI: [10.1246/cl.2001.286](https://doi.org/10.1246/cl.2001.286).
- 42 Y.-L. Zhao, L. Liu, W. Zhang, C.-H. Sue, Q. Li, O. Š. Miljanić, O. M. Yaghi and J. F. Stoddart, *Chem. – Eur. J.*, 2009, **15**, 13356–13380.



- 43 A. R. McDonald, N. Franssen, G. P. M. van Klink and G. van Koten, *J. Organomet. Chem.*, 2009, **694**, 2153–2162.
- 44 M. Taniguchi, J. S. Lindsey, D. F. Bocian and D. Holten, *J. Photochem. Photobiol., C*, 2021, **46**, 100401.
- 45 J. Parkash, J. H. Robblee, J. Agnew, E. Gibbs, P. Collings, R. F. Pasternack and J. C. de Paula, *Biophys. J.*, 1998, **74**, 2089–2099.
- 46 R. F. Pasternack and P. J. Collings, *Science*, 1995, **269**, 935–939.
- 47 A. Rodger and J. J. Chubb, *Encyclopedia of Analytical Chemistry*, 2023, pp. 1–42, DOI: [10.1002/9780470027318.a5402.pub3](https://doi.org/10.1002/9780470027318.a5402.pub3).
- 48 J. R. Lakowicz, *Principles of Fluorescence Spectroscopy*, Kluwer Academic/Plenum Publishers, New York, 1999.

